
PET/CT Imaging of Unstable Carotid Plaque with ^{68}Ga -Labeled Somatostatin Receptor Ligand

Ming Young Simon Wan¹, Raymond Endozo¹, Sofia Michopoulou¹, Robert Shortman¹, Manuel Rodriguez-Justo², Leon Menezes¹, Syed Yusuf³, Toby Richards⁴, Damian Wild⁵, Beatrice Waser⁶, Jean Claude Reubi⁶, and Ashley Groves¹

¹Institute of Nuclear Medicine, University College London, London, United Kingdom; ²Department of Histopathology, University College London, London, United Kingdom; ³Department of Vascular Surgery, Brighton and Sussex University Hospitals, Sussex, United Kingdom; ⁴Department of Vascular Surgery, University College London, London, United Kingdom; ⁵Division of Nuclear Medicine, University of Basel Hospital, Basel, Switzerland; and ⁶Cell Biology and Experimental Cancer Research, Institute of Pathology, University of Berne, Berne, Switzerland

^{68}Ga -labeled somatostatin receptor ligand PET imaging has recently been shown in preclinical and early human studies to have a potential role in the evaluation of vulnerable arterial plaques. We prospectively evaluated carotid plaque ^{68}Ga -DOTATATE uptake in patients with recent carotid events, assessed inter- and intraobserver variability of such measurements, and explored the mechanism of any plaque DOTATATE activity with immunohistochemistry in resected specimens. **Methods:** Twenty consecutively consenting patients with recent symptomatic carotid events (transient ischemic attack, stroke, or amaurosis fugax), due for carotid endarterectomy, were prospectively recruited. ^{68}Ga -DOTATATE PET/CT of the neck was performed before surgery. ^{68}Ga -DOTATATE uptake was measured by drawing regions of interest along the carotid plaques and contralateral plaques/carotid arteries by an experienced radionuclide radiologist and radiographer. Two PET quantification methods with inter- and intraobserver variability were assessed. Resected carotid plaques were retrieved for somatostatin receptor subtype-2 (sst2) immunohistochemical staining. **Results:** The median time delay between research PET and surgery was 2 d. SUVs and target-to-background ratios for the symptomatic plaques and the asymptomatic contralateral carotid arteries/plaques showed no significant difference ($n = 19$, $P > 0.10$), regardless of quantification method. The intraclass correlation coefficient was greater than 0.8 in all measures of carotid artery/plaque uptake (SUV) and greater than 0.6 in almost all measures of target-to-background ratio. None of the excised plaques was shown to contain cells (macrophages, lymphocytes, vessel-associated cells) expressing sst2 on their cell membrane. **Conclusion:** ^{68}Ga -DOTATATE activity on PET in recently symptomatic carotid plaques is not significantly different from contralateral carotids/plaques. Any activity seen on PET is not shown to be from specific sst2 receptor-mediated uptake in vitro. It is therefore unlikely that sst2 PET/CT imaging will have a role in the detection and characterization of symptomatic carotid plaques.

Key Words: somatostatin; PET/CT; DOTATATE; carotid; vulnerable plaques

J Nucl Med 2017; 58:774–780

DOI: 10.2967/jnumed.116.181438

Received Jul. 21, 2016; revision accepted Oct. 4, 2016.
For correspondence or reprints contact: Ming Young Simon Wan, Institute of Nuclear Medicine, T5, University College Hospital, London, U.K., NW2 1BU.
E-mail: mwan@nhs.net
Published online Dec. 8, 2016.
COPYRIGHT © 2017 by the Society of Nuclear Medicine and Molecular Imaging.

Atherosclerosis is a leading cause of mortality and morbidity. There is the concept that although atherosclerotic plaques may contribute to symptoms by luminal stenosis, it is the disruption of unstable plaques that leads to catastrophic events, including stroke and myocardial infarction. Termed *vulnerable plaques*, these unstable plaques are believed to have characteristic features such as inflammatory cell infiltration, lipid cores, and fibrous caps (1,2).

Measuring the degree of luminal stenosis was the mainstay of assessment and directed management decisions until recently (3–5). Recognition of this method's limitation has driven the use of biomarkers, such as fractional flow reserve, in coronary disease and exploration of functional imaging to noninvasively identify vulnerable plaques (6,7).

Radionuclide imaging has the advantageous capability of directly probing molecular mechanisms in vivo using radioactive tracers (8). In particular, the assessment of plaque inflammation using ^{18}F -FDG PET/CT has been extensively studied. Since early validation studies (9,10), plaque ^{18}F -FDG uptake has been associated with cardiovascular risk factors and circulating inflammatory markers (11,12). ^{18}F -FDG uptake can predict future cardiovascular risk in asymptomatic individuals (13) and early stroke recurrence (14). Further studies have shown the potential of ^{18}F -FDG uptake in evaluating treatment response with statins (15). Moreover, ^{18}F -FDG PET has become the primary endpoint in some drug trials assessing the drugs' anti-inflammatory effect (16,17). Despite the success, extension of its use to coronary vessels is limited by variably high background myocardial ^{18}F -FDG activity. This has fueled motivation to explore alternative PET tracers (18).

Inflammatory cells involved in the pathophysiology of atherosclerosis (19) may express somatostatin receptors (20,21). It is also known that vessels can express somatostatin receptors under certain conditions (22,23). Recently, 2 preclinical murine studies have demonstrated the potential of somatostatin receptor PET in atherosclerosis imaging (24,25). Retrospective human studies with these tracers have also shown promise (26–29). In this study, we prospectively explored the use of a clinically established PET tracer, ^{68}Ga -DOTATATE, a somatostatin receptor ligand, in patients who are believed to have vulnerable carotid plaques, based on recent symptomatic events. We hypothesized that ^{68}Ga -DOTATATE uptake is measurably higher on PET/CT in vulnerable carotid plaques than in contralateral carotid arteries/plaques. We assessed 2 quantification methods, adapted from previous carotid PET tracer-histologic validation studies.

Interobserver and intraobserver agreement were tested. As a secondary imaging endpoint, we studied the relationship of PET uptake with plaque composition on CT angiogram (CTA). CTA has been shown to correlate well with histology (30). Finally, we studied the subsequently excised carotid endarterectomy samples with emphasis on somatostatin subtype-2 (sst2) immunohistochemistry.

MATERIALS AND METHODS

Patients

The institutional review board approved this study. All subjects signed a written informed consent form. Twenty consecutive consenting patients were recruited. Inclusion criteria were patients planned for carotid endarterectomy for recent symptomatic events (stroke, transient ischemic attack, or amaurosis fugax). They were identified from a well-established regional hyperacute stroke unit and transient ischemic attack clinics. As per local routine, the diagnosis was confirmed by specialist stroke physicians. Other potential mechanisms of these symptoms were reasonably excluded. These patients had greater than 70% carotid stenosis confirmed by 2 concordant imaging modalities of CTA down to aortic arch, MR angiogram or duplex ultrasound. These were interpreted by local experts using the European Carotid Surgery Trial and North American Symptomatic Carotid Endarterectomy grading for carotid stenosis (4,5). The patients' management was fully discussed at multidisciplinary board meetings attended by specialist stroke physicians, vascular surgeons, and neuroradiologists. Here, the etiology of the presumed carotid events was scrutinized. Consensus was made in this forum that vulnerable carotid plaque was the likely culprit and that the patient was deemed at high risk for further events. A plan for carotid endarterectomy was agreed on during the forum. Only cases clearly attributed to the carotid and high risk were considered for this study. Exclusion criteria were age younger than 45 y, pregnancy and lactation, and inability to consent.

Imaging

All patients underwent ^{68}Ga -DOTATATE PET/CT before surgery. An additional CTA was performed at the same time for superior coregistration of ^{68}Ga -DOTATATE uptake and carotid plaque, unless precluded by renal failure.

Synthesis and labeling of ^{68}Ga -DOTATATE has been published previously (31). Our radiopharmacy has an average radiochemical purity of 99% (range, 98%–99.9%) for this tracer. Patients were given ^{68}Ga -DOTATATE injection (mean activity received, 157 MBq) with an uptake time of 60 min. All PET/CT images were obtained on the same scanner (DiscoveryVCT; GE Healthcare). A single-bed-position acquisition was performed to image the carotid arteries. CT parameters were 120 kVp, mA modulation of 30–300 mAs, noise index of 20, pitch of 1.375, rotation time of 800 ms, pixel size of 0.98 mm, and slice thickness of 2.5 mm. This acquisition was followed by an emission scan with 3-dimensional acquisition over 4 min, iterative reconstruction (ordered-subset expectation maximization, 20 subsets, 2 iterations), 3.27-mm slice thickness, and 5.5-mm pixel size. Attenuation correction was performed with the noncontrast CT. CTA was performed as published previously (32).

PET Analysis

There is no established method for quantification of ^{68}Ga -DOTATATE PET in this context. We drew on previous published carotid PET tracer-histologic validation studies for the 2 methods used (10,32,33). Images were analyzed using Xeleris (GE Healthcare). Carotid plaques were identified using CTA as part of this study or in a few patients with renal failure, from imaging acquired at the time of their acute presentation days before the research PET/CT. The location of the carotid plaques on PET was identified by either fusing the PET and CTA images or by

reviewing the imaging side by side. Plaque uptake was measured by drawing regions of interest (ROIs) around the carotid arteries at every slice, where plaques were visible, and around the carotid bifurcation (up to 2 cm superior and 1 cm inferior to the bifurcation). If no clear plaque was seen on a given slice (as was often the case on the asymptomatic side, on eventual unmasking of the interpreter), an ROI was placed around the carotid arteries at the same axial slices as any contralateral carotid plaque to allow comparison. In each ROI, the SUV_{mean} and SUV_{max} were calculated (Bq/mL). Average blood-pool activity for each patient was derived from averaging at least 3 different ROIs in venous structures, usually at the most distended segment of the jugular vein. Measurements from the ROI were computed in 2 different ways to reflect 2 different quantification methods of ^{68}Ga -DOTATATE uptake. One method used was the volume plaque method: mean and maximum pixel activities for the ROI in all the slices in a plaque/vessel defined above were averaged to give SUV_{mean} and SUV_{max} of the plaques. These were also corrected for blood-pool activity, by division by the average blood-pool activity, to derive target-to-background ratio (TBR) measurements: TBR_{mean} and TBR_{max} . A second method used was the most intense pixel/ROI method: the single pixel with the most intense signal and the ROI with the most intense averaged SUV in a plaque/vessel were selected. These were designated $\text{maxSUV}_{\text{max}}$ and $\text{maxSUV}_{\text{mean}}$. These were corrected for blood-pool activity as above to derive $\text{maxTBR}_{\text{max}}$ and $\text{maxTBR}_{\text{mean}}$.

Inter- and Intraobserver Variability

To assess intraobserver variability, PET analysis was performed twice by interpreter 1, a PET-accredited radiologist with interest in cardiovascular imaging, with an 8-wk period in between. Interobserver variability was assessed by a further analysis by interpreter 2, a superintendent radiographer with prior experience in similar carotid PET quantification. The 2 interpreters coread several pilot studies (not included in this study) to establish a standard protocol for analysis. All images were analyzed with the interpreters masked to the side of symptoms.

Plaque Composition Analysis

Carotid plaques on the symptomatic side were manually segmented slice by slice on the CTA using an ADW (GE Healthcare) workstation. The lumen was segmented out manually. Plaque composition in individual pixels was assigned based on density (Hounsfield units of 20–60 were assigned as lipid, 60–130 as fibrous, and >130 as calcification) (32,34). Plaque components were expressed as percentage of overall plaque volume.

Histologic Analysis

All patients proceeded to undergo carotid endarterectomy using an eversion endarterectomy technique, performed by 1 of 3 dedicated surgeons on the next-available list. Plaques were immediately fixed in 10% buffered formalin and decalcified following the standard protocol at University College London Hospitals. Specimens were transversely sectioned at 5-mm intervals, embedded face up in paraffin, and cut at 3- to 4- μm thickness. Hematoxylin and eosin sections were obtained, and the plaque was typed according to American Heart Association criteria (2). Pan-macrophage marker immunostaining (CD68) was performed as previously described (32).

sst2 immunohistochemistry was performed at the University of Berne, where there is established expertise in somatostatin immunohistochemistry, as previously published using the sst2 antibody UMB1 (35). Tissues known to express sst2 (neuroendocrine tumors, germinal centers, and peritumoral vessels) were used as positive controls (21,23). sst2 immunohistochemistry was selected because ^{68}Ga -DOTATATE is known to be highly selective for sst2 labeling (36). There is no reason to believe that it would label another somatostatin receptor subtype in these tissues. Samples were sent from London to Berne in batches, with

10 randomly selected samples initially, followed by batches of 3 specifically selected for their highest ⁶⁸Ga-DOTATATE signals on PET/CT.

Statistical Analysis

Statistical tests were performed using SPSS (version 21; IBM Corp.). Statistical significance was assigned for a *P* value of less than 0.05. Normality of measurements was tested with the Shapiro–Wilk test and visual inspection. The 2-tailed paired-sample *t* test was used to compare uptake between the symptomatic and asymptomatic sides. The intraclass correlation coefficient was used to assess intraobserver variability (1-way random-effects model with absolute agreement) and interobserver variability (2-way mixed-effects model with absolute agreement) (37). The Spearman rank correlation was used to assess the relationship of PET signal with CT plaque components and the Kruskal–Wallis test for the relationship of immunohistochemistry with PET signal.

RESULTS

Patient demographics, risk factors, and medications are presented in Table 1. All excised symptomatic plaques were considered advanced by American Heart Association histologic criteria (type V or VI). Detailed histologic features are presented in Supplemental Table 1 (supplemental materials are available at <http://jnm.snmjournals.org>).

Imaging Findings

One patient had focal intense uptake in the asymptomatic carotid bifurcation, corresponding to a previously undiagnosed carotid body tumor. This patient was excluded. There was no statistically significant difference between symptomatic carotid plaques and asymptomatic carotid plaques/arteries (Fig. 1) in any of the SUV and TBR measurements (Table 2; Fig. 2; Supplemental Figs. 1 and 2).

All values for SUV measurements were greater than 0.9, with narrow confidence intervals, indicating excellent agreement. Values for TBR measurements were almost exclusively greater than 0.6, indicating substantial agreement (Supplemental Table 2).

There was no statistically significant correlation between any SUV and TBR parameters with the CT plaque composition parameters (Supplemental Table 3).

Immunohistochemistry Findings

Variable CD68 staining was observed in the excised plaques, at values comparable to previous carotid plaque imaging–histologic investigations (Supplemental Table 1) (32). There was no statistically significant relationship of CD68 with any SUV and TBR parameters (Supplemental Table 4).

None of the tissues was shown to contain cells expressing sst2 on their cell membrane (Fig. 3), a major criterion for G-protein–coupled receptor specificity (28). Moreover, no nonspecific labeling, that is, no cytoplasmic staining of the cells, was detected in the analyzed tissues.

DISCUSSION

In this prospective study of ⁶⁸Ga-DOTATATE PET/CT with histologic validation of human vulnerable carotid plaques, we addressed the pertinent question of whether sst2-expressing cells (believed to be macrophages) are present in these plaques, in sufficient density for detection with ⁶⁸Ga-DOTATATE PET/CT *in vivo*. We demonstrated that measurement of vascular uptake with ⁶⁸Ga-DOTATATE PET/CT in carotid plaques was feasible, using

TABLE 1
Patient Characteristics

Characteristic	Value
Mean age ± SD (y)	78.5 ± 9.5
Sex (male:female)	12:8
Median time between symptom to PET/CT (d)	6.5 (range, 2–27)
Median time between PET/CT to endarterectomy (d)	2 (range, 0–6)
Diagnosis (%)	
Stroke	40
Transient ischemic attack	30
Amaurosis fugax	30
Cardiovascular risk factors (%)	
Hypertension	85
Smoker	45
Previous transient ischemic attack/stroke	35
Previous ischemic heart disease	40
Diabetes	30
Atrial fibrillation	15
Hypercholesterolemia	65
Medication at presentation (%)	
Aspirin	40
Clopidogrel	10
Warfarin	10
Statins	55
Ezetimibe	15

2 different PET quantification methods, with both showing substantial to excellent agreements. However, we did not find significantly higher ⁶⁸Ga-DOTATATE activity in vulnerable carotid plaques than contralateral carotids/plaques. sst2 immunohistochemistry was chosen for its established, direct relevance to ⁶⁸Ga-DOTATATE sst2 binding at the cell surface (in contrast to messenger RNA/polymerase chain reaction or macrophage cluster of differentiation markers). Despite confirmation of the presence of CD68-positive macrophages, none of the excised plaques examined showed cells expressing sst2 on their cell membrane, indicating that there is no molecular basis for an sst2 receptor–mediated uptake of somatostatin tracer *in vitro* in acute human plaques. Our findings would not support the use of ⁶⁸Ga-DOTATATE in the detection and characterization of vulnerable plaques in human.

Rationale for Study of ⁶⁸Ga-DOTATATE in Atherosclerosis

Monocytes and macrophages were the first inflammatory cells to be associated with atherosclerosis. They are believed to play important roles in its pathogenesis, contributing to necrotic core formation and fibrous cap thinning in advanced atherosclerosis, features thought to confer vulnerability (19,38). It is known that human macrophages express sst2 on their cell surface in cell culture experiments (20,39). ⁶⁸Ga-DOTATATE, a specific sst2 receptor agonist, therefore was thought to have the potential to be a surrogate marker of inflammation to study plaque biology. This has been recently validated in 2 preclinical murine experiments (apolipoprotein –/– mice model) at a tissue level (24,25).

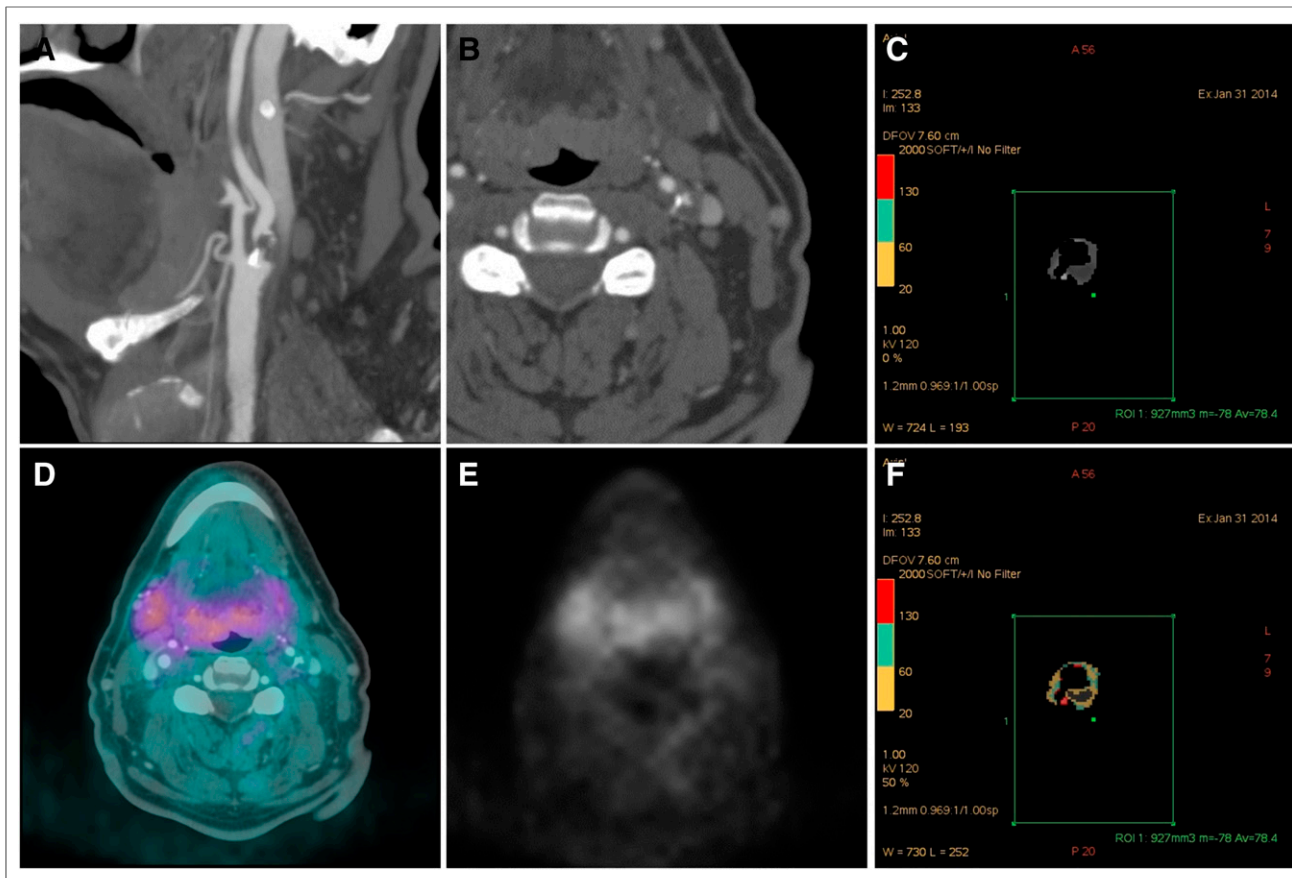


FIGURE 1. Images from 68-y-old man with multiple recent left amaurosis fugax. (A and B) CTA shows severe stenosis of left internal carotid artery extending from bifurcation. (D and E) Fused and PET image at this level. (C and F) Segmented plaque on CTA from a different level, with color-coded scale showing plaque compositions.

Human Studies with Somatostatin Receptor PET

Four recent studies examined the potential role of these in atherosclerosis, retrospectively in patients with neuroendocrine tumors.

One found significant correlation between TBR with calcific plaque burden and prior vascular events (26). Another found that TBR at areas of focal vessel uptake are higher in patients with more cardiovascular risk factors (27). A further study found increased ^{68}Ga -DOTATATE uptake in coronary plaques compared with normal coronary segments (28). The last compared ^{68}Ga -DOTATOC and ^{64}Cu -DOTATATE (29), in correlating vessel uptake against cardiovascular risk factors. ^{64}Cu -DOTATATE demonstrated a higher uptake than ^{68}Ga -DOTATOC, with positive correlation with Framingham scores only with ^{64}Cu -DOTATATE but not with ^{68}Ga -DOTATOC.

To our knowledge, there has been 1 prospective study specifically looking at vulnerable plaque (40). This examined 10 patients with stroke or transient ischemic attack with ^{64}Cu -DOTATATE. The authors found a higher uptake in the symptomatic plaque than in the contralateral carotid vessel. Significant but weak association was demonstrated between uptake on PET and CD163 and CD68 gene expression in endarterectomy samples on univariate analysis, with CD163 remaining significant on multivariate analysis. CD163 is believed to be a marker of M2 (alternatively activated) macrophages, found in hemorrhagic zones of plaques, and possibly has an antiinflammatory function.

Interpretation in Context of Published Literature

The preclinical promise has not translated into a positive result in our study. A plausible explanation may be species-specific variability of somatostatin receptor subtype expression. For instance, human

TABLE 2
SUV and TBR Between Symptomatic and Asymptomatic Sides

Method	Parameter							
	SUV _{max}	SUV _{mean}	TBR _{max}	TBR _{mean}	maxSUV _{max}	maxSUV _{mean}	maxTBR _{max}	maxTBR _{mean}
Volume plaque, <i>P</i> value	0.223	0.784	0.507	0.707				
Most intense pixel/ROI, <i>P</i> value					0.098	0.897	0.248	0.810

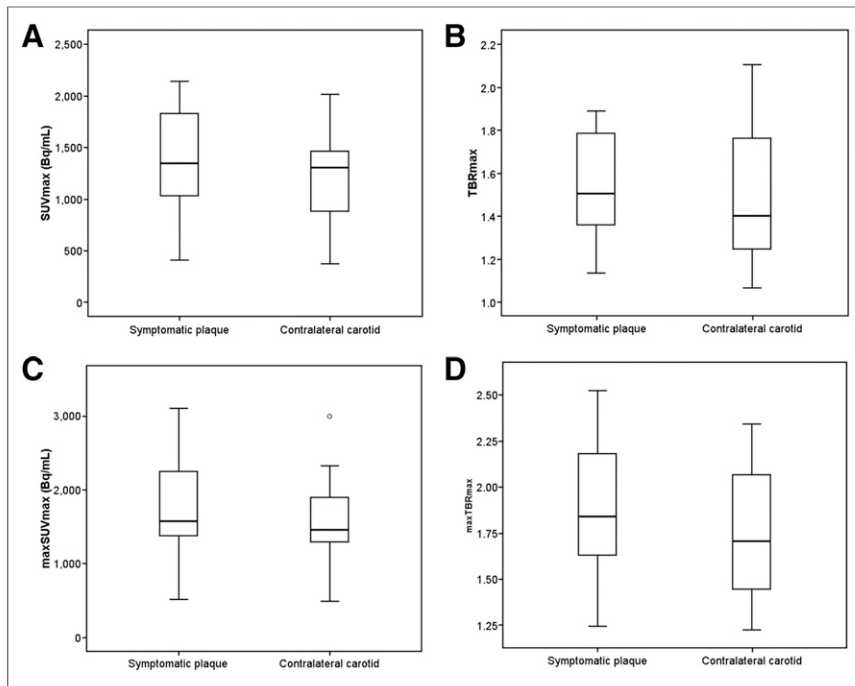


FIGURE 2. Box whisker plots showing no significant difference in SUV and TBR parameters between symptomatic and asymptomatic side.

chronic atherosclerotic popliteal arteries were found to show consistently higher *sst1* expression than *sst2* or *sst4*, which differed from the predominant *sst2* and *sst3* expression in rat vessels (41). In addition, although macrophage activation is a feature of inflammation

therefore raises serious questions about the meaning of any observed ^{68}Ga -DOTATATE (and ^{18}F -FDG) signal. The only published prospective study on ^{64}Cu -DOTATATE did not examine *sst2* expression in the resected tissue (40).

in atherosclerosis development, there are conflicting results in the published preclinical human cell experiments as to whether *sst2* expression on macrophages signifies their activation (20,25,39). Our validation on human vulnerable plaques is more directly relevant to clinical practice. Our results would suggest a lack of significant *sst2* expression in macrophages present in recently symptomatic plaques.

Our study also adds to the current knowledge in that unlike our study, the retrospective studies mentioned above (26–29) did not allow study of causation, or molecular mechanism of any observed tracer activity, to the clinical parameters observed. These studies were also performed in patients with chronic plaques only. ^{18}F -FDG uptake has been shown to evolve over the chronic course of disease (42). It is likely that ^{68}Ga -DOTATATE uptake would behave similarly. One of the retrospective studies (27) showed poor colocalization of ^{18}F -FDG and ^{68}Ga -DOTATATE signal in vessels. ^{18}F -FDG activity in plaques is established as a surrogate marker of plaque inflammation, validated against macrophage cell surface marker (CD68) in several studies (9,10). Poor colocalization of the ^{68}Ga -DOTATATE and ^{18}F -FDG signal

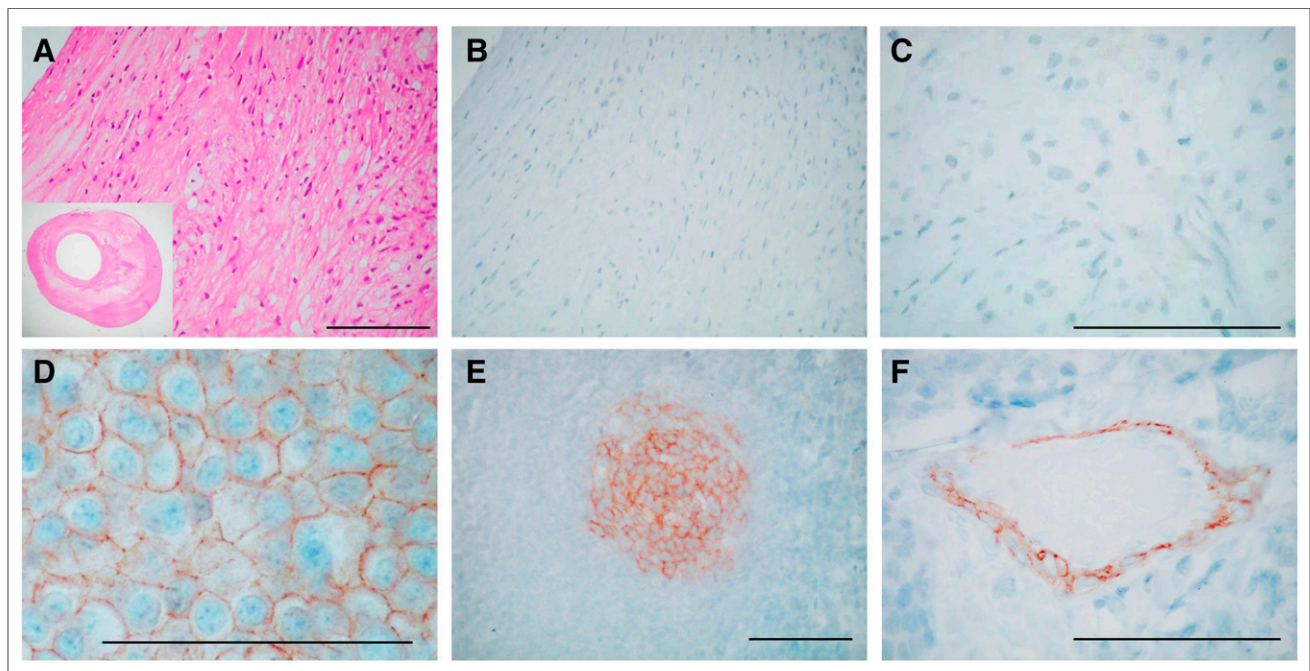


FIGURE 3. *sst2* immunohistochemistry showing absence of *sst2* in representative carotid plaque. (A) Hematoxylin and eosin staining of representative part of plaque (insert shows whole plaque). (B) *sst2* immunohistochemistry of adjacent section showing absence of *sst2*. (C) *sst2* immunohistochemistry at higher magnification. (D–F) Positive *sst2* immunohistochemistry in 3 different reference control tissues. (D) Neuroendocrine tumor cells. (E) Lymphocytes in gut germinal center. (F) Endothelial cells in peritumoral vessel. Bars = 0.1 mm.

Taken together, it is likely that there are complex relationships between stage of plaque evolution (chronic vs. acute), macrophage density and activity, somatostatin receptor subtype expression, ^{18}F -FDG, and somatostatin receptor PET signal. Macrophage subtype/activation in vulnerable human atherosclerosis plaques has been studied recently in vitro, generally showing a higher expression of proinflammatory M1 macrophages than M2 macrophages, which may be antiatherogenic (43–45). How this variation of macrophage expression profile interacts with ^{68}Ga -DOTATATE signal needs to be further explored.

Our sample size was small and this raises the possibility of a false-negative study. However, our negative imaging findings were supported by robust histologic examination of ex vivo samples, performed in a laboratory with long-held expertise in somatostatin receptor studies. The antibodies used were the current gold standard of sst2 immunostaining, which has been extensively evaluated previously (35,46). Moreover, our sample size was comparable to other similar carotid imaging–histologic validation investigations (10,18,33). There is heterogeneity of time between carotid event, research PET, and endarterectomy in our patients, reflecting the logistic challenge surrounding patient recruitment and tracer, scanner, and operating theater availability. However, the ranges of delay are comparable with similar studies. We performed single-time-point imaging at 60 min only. The bulk of the retrospective data on vascular DOTATATE PET uptake had similar uptake time. In addition, an early scan (median, 85 min) with ^{64}Cu -DOTATATE has already been shown to be preferred, compared with delayed acquisition (40).

^{68}Ga has less optimal imaging characteristics compared with ^{18}F or ^{64}Cu . ^{68}Ga -DOTATATE may be less sensitive to weak differences in uptake compared with the equivalent ^{64}Cu -labeled tracers (29). Higher image noise is reflected by poorer inter- and intraobserver agreement of TBR measurements despite demonstrated excellent agreement in SUV measurements. This is because while arterial plaques provide a clear target for directing ROI placement, ROIs for blood pool may be more operator dependent. Therefore, image noise and variation in blood-pool measurements manifest as poorer TBR agreement. Increasing acquisition time beyond 4 min may counter this, but at the expense of risk of detrimental patient movement and misregistration.

Spillover and partial-volume effect from adjacent structures is a concern, with major salivary glands and thyroid shown to have an SUV_{max} of 2.3–4.2 (31), higher than vascular activity observed. There may also be increased activity in adjacent nodes. ROIs were drawn carefully to minimize these.

CONCLUSION

We demonstrated the feasibility of ^{68}Ga -DOTATATE measurement of carotid plaques on PET/CT. However, we found no significant difference in ^{68}Ga -DOTATATE activity in symptomatic carotid plaques compared with the asymptomatic side. This finding was supported by the compelling lack of sst2 expression on excised plaques. Our findings indicate no molecular basis for an sst2 receptor-mediated uptake of the somatostatin tracer in vitro and would not support the use of ^{68}Ga -DOTATATE PET in assessment of acute vulnerable human plaques.

DISCLOSURE

This work was partially undertaken at UCLH/UCL, which received a proportion of funding from the Department of Health's NIHR Biomedical Research Centre's funding scheme. No other potential conflict of interest relevant to this article was reported.

REFERENCES

- Shah PK. Mechanisms of plaque vulnerability and rupture. *J Am Coll Cardiol*. 2003;41:15S–22S.
- Stary HC, Chandler AB, Dinsmore RE, et al. A definition of advanced types of atherosclerotic lesions and a histological classification of atherosclerosis: a report from the Committee on Vascular Lesions of the Council on Arteriosclerosis, American Heart Association. *Arterioscler Thromb Vasc Biol*. 1995;15:1512–1531.
- Boden WE, O'Rourke RA, Teo KK, et al. Optimal medical therapy with or without PCI for stable coronary disease. *N Engl J Med*. 2007;356:1503–1516.
- Randomised trial of endarterectomy for recently symptomatic carotid stenosis: final results of the MRC European Carotid Surgery Trial (ECST). *Lancet*. 1998;351:1379–1387.
- North American Symptomatic Carotid Endarterectomy Trial Collaborators. Beneficial effect of carotid endarterectomy in symptomatic patients with high-grade carotid stenosis. *N Engl J Med*. 1991;325:445–453.
- Nicolaides AN, Kakkos SK, Kyriacou E, et al. Asymptomatic internal carotid artery stenosis and cerebrovascular risk stratification. *J Vasc Surg*. 2010;52:1486–1496.e1.
- De Bruyne B, Pijls NH, Kalesan B, et al. Fractional flow reserve-guided PCI versus medical therapy in stable coronary disease. *N Engl J Med*. 2012;367:991–1001.
- Evans NR, Tarkin JM, Chowdhury MM, Warburton EA, Rudd JH. PET imaging of atherosclerotic disease: advancing plaque assessment from anatomy to pathophysiology. *Curr Atheroscler Rep*. 2016;18:30.
- Rudd JHF. Imaging atherosclerotic plaque inflammation with [^{18}F]-fluorodeoxyglucose positron emission tomography. *Circulation*. 2002;105:2708–2711.
- Tawakol A, Migrino RQ, Bashian GG, et al. In vivo ^{18}F -fluorodeoxyglucose positron emission tomography imaging provides a noninvasive measure of carotid plaque inflammation in patients. *J Am Coll Cardiol*. 2006;48:1818–1824.
- Yoo HJ, Kim S, Park MS, et al. Vascular inflammation stratified by C-reactive protein and low-density lipoprotein cholesterol levels: analysis with ^{18}F -FDG PET. *J Nucl Med*. 2011;52:10–17.
- Noh TS, Moon SH, Cho YS, et al. Relation of carotid artery ^{18}F -FDG uptake to C-reactive protein and Framingham risk score in a large cohort of asymptomatic adults. *J Nucl Med*. 2013;54:2070–2076.
- Figuerola AL, Abdelbaky A, Truong QA, et al. Measurement of arterial activity on routine FDG PET/CT images improves prediction of risk of future CV events. *JACC Cardiovasc Imaging*. 2013;6:1250–1259.
- Marnane M, Merwick A, Sheehan OC, et al. Carotid plaque inflammation on ^{18}F -fluorodeoxyglucose positron emission tomography predicts early stroke recurrence. *Ann Neurol*. 2012;71:709–718.
- Tahara N, Kai H, Ishibashi M, et al. Simvastatin attenuates plaque inflammation: evaluation by fluorodeoxyglucose positron emission tomography. *J Am Coll Cardiol*. 2006;48:1825–1831.
- Comparison of clopidogrel versus ticagrelor therapy for atherosclerotic plaque inflammation. ClinicalTrials.gov website. <https://clinicaltrials.gov/ct2/show/NCT01905566>. Accessed January 12, 2017.
- The effect(s) of sevelamer carbonate (renvela) on atherosclerotic plaque inflammation judged by FDG-PET scan. ClinicalTrials.gov website. <https://clinicaltrials.gov/ct2/show/NCT01238588>. Accessed January 12, 2017.
- Joshi NV, Vesey AT, Williams MC, et al. ^{18}F -fluoride positron emission tomography for identification of ruptured and high-risk coronary atherosclerotic plaques: a prospective clinical trial. *Lancet*. 2014;383:705–713.
- Moore KJ, Tabas I. Macrophages in the pathogenesis of atherosclerosis. *Cell*. 2011;145:341–355.
- Armani C, Catalani E, Balbarini A, Bagnoli P, Cervia D. Expression, pharmacology, and functional role of somatostatin receptor subtypes 1 and 2 in human macrophages. *J Leukoc Biol*. 2007;81:845–855.
- Reubi JC, Horisberger U, Kappeler A, Laissue JA. Localization of receptors for vasoactive intestinal peptide, somatostatin and substance p in distinct compartments of human lymphoid organs. *Blood*. 1998;92:191–197.
- Reubi JC, Mazzucchelli L, Laissue JA. Intestinal vessels express a high density of somatostatin receptors in human inflammatory bowel disease. *Gastroenterology*. 1994;106:951–959.
- Reubi JC, Mazzucchelli L, Hennig I, Laissue JA. Local upregulation of neuro-peptide receptors in host blood vessels around human colorectal cancers. *Gastroenterology*. 1996;110:1719–1726.
- Rinne P, Hellberg S, Kiugel M, et al. Comparison of somatostatin receptor 2-targeting PET tracers in the detection of mouse atherosclerotic plaques. *Mol Imaging Biol*. 2016;18:99–108.
- Li X, Bauer W, Kreissl MC, et al. Specific somatostatin receptor II expression in arterial plaque: ^{68}Ga -DOTATATE autoradiographic, immunohistochemical and flow cytometric studies in apoE-deficient mice. *Atherosclerosis*. 2013;230:33–39.

26. Rominger A, Saam T, Vogl E, et al. In vivo imaging of macrophage activity in the coronary arteries using ⁶⁸Ga-DOTATATE PET/CT: correlation with coronary calcium burden and risk factors. *J Nucl Med*. 2010;51:193–197.
27. Li X, Sannick S, Lapa C, et al. ⁶⁸Ga-DOTATATE PET/CT for the detection of inflammation of large arteries: correlation with ¹⁸F-FDG, calcium burden and risk factors. *EJNMMI Res*. 2012;2:52.
28. Mojtahedi A, Alavi A, Thamake S, et al. Assessment of vulnerable atherosclerotic and fibrotic plaques in coronary arteries using ⁶⁸Ga-DOTATATE PET/CT. *Am J Nucl Med Mol Imaging*. 2014;5:65–71.
29. Malmberg C, Ripa RS, Johnbeck CB, et al. ⁶⁴Cu-DOTATATE for noninvasive assessment of atherosclerosis in large arteries and its correlation with risk factors: head-to-head comparison with ⁶⁸Ga-DOTATOC in 60 patients. *J Nucl Med*. 2015;56:1895–1900.
30. de Weert TT, Ouhous M, Meijering E, et al. In vivo characterization and quantification of atherosclerotic carotid plaque components with multidetector computed tomography and histopathological correlation. *Arterioscler Thromb Vasc Biol*. 2006;26:2366–2372.
31. Shastry M, Kayani I, Wild D, et al. Distribution pattern of ⁶⁸Ga-DOTATATE in disease-free patients. *Nucl Med Commun*. 2010;31:1025–1032.
32. Menezes LJ, Kotze CW, Agu O, et al. Investigating vulnerable atheroma using combined ¹⁸F-FDG PET/CT angiography of carotid plaque with immunohistochemical validation. *J Nucl Med*. 2011;52:1698–1703.
33. Beer AJ, Pelisek J, Heider P, et al. PET/CT imaging of integrin alphavbeta3 expression in human carotid atherosclerosis. *JACC Cardiovasc Imaging*. 2014;7:178–187.
34. Homburg PJ, Rozie S, van Gils MJ, et al. Association between carotid artery plaque ulceration and plaque composition evaluated with multidetector CT angiography. *Stroke*. 2011;42:367–372.
35. Körner M, Waser B, Schonbrunn A, Perren A, Reubi JC. Somatostatin receptor subtype 2A immunohistochemistry using a new monoclonal antibody selects tumors suitable for in vivo somatostatin receptor targeting. *Am J Surg Pathol*. 2012;36:242–252.
36. Reubi JC, Schar JC, Waser B, et al. Affinity profiles for human somatostatin receptor subtypes SST1–SST5 of somatostatin radiotracers selected for scintigraphic and radiotherapeutic use. *Eur J Nucl Med*. 2000;27:273–282.
37. McGraw KO, Wong SP. Forming inferences about some intraclass correlation coefficients. *Psychol Methods*. 1996;1:30–46.
38. Woollard KJ, Geissmann F. Monocytes in atherosclerosis: subsets and functions. *Nat Rev Cardiol*. 2010;7:77–86.
39. Dalm VASH, van Hagen PM, Van Koetsveld PM, et al. Expression of somatostatin, cortistatin, and somatostatin receptors in human monocytes, macrophages, and dendritic cells. *Am J Physiol Endocrinol Metab*. 2003;285:E344–E353.
40. Pedersen SF, Sandholt BV, Keller SH, et al. ⁶⁴Cu-DOTATATE PET/MRI for detection of activated macrophages in carotid atherosclerotic plaques studies in patients undergoing endarterectomy. *Arterioscler Thromb Vasc Biol*. 2015;35:1696–1703.
41. Curtis SB, Hewitt J, Yakubovitz S, Anzarut A, Hisang YN, Buchan AMJ. Somatostatin receptor subtype expression and function in human vascular tissue. *Am J Physiol Heart Circ Physiol*. 2000;278:H1815–H1822.
42. Menezes LJ, Kayani I, Ben-Haim S, Hutton B, Ell PJ, Groves AM. What is the natural history of ¹⁸F-FDG uptake in arterial atheroma on PET/CT? Implications for imaging the vulnerable plaque. *Atherosclerosis*. 2010;211:136–140.
43. Shaikh S, Brittenden J, Lahiri R, Brown PA, Thies F, Wilson HM. Macrophage subtypes in symptomatic carotid artery and femoral artery plaques. *Eur J Vasc Endovasc Surg*. 2012;44:491–497.
44. Cho KY, Miyoshi H, Kuroda S, et al. The phenotype of infiltrating macrophages influences arteriosclerotic plaque vulnerability in the carotid artery. *J Stroke Cerebrovasc Dis*. 2013;22:910–918.
45. Medbury HJ, Williams H, Fletcher JP. Clinical significance of macrophage phenotypes in cardiovascular disease. *Clin Transl Med*. 2014;3:63.
46. Fischer T, Doll C, Jacobs S, Kolodziej A, Stumm R, Schulz S. Reassessment of sst2 somatostatin receptor expression in human normal and neoplastic tissues using the novel rabbit monoclonal antibody UMB-1. *J Clin Endocrinol Metab*. 2008;93:4519–4524.